HXeCCH in Ar and Kr matrices

Hanna Tanskanen,[a] Leonid Khriachtchev, Jan Lundell, and Markku Räsänen
Department of Chemistry, University of Helsinki, P.O. Box 55, Helsinki FIN-00014, Finland

(Received 24 May 2006; accepted 14 June 2006; published online 15 August 2006)

HXeCCH molecule is prepared in Ar and Kr matrices and characterized by IR absorption spectroscopy. The experiments show that HXeCCH can be made in another host than the polarizable Xe environment. The H–Xe stretching absorption of HXeCCH in Ar and Kr is blueshifted from the value measured in solid Xe. The maximum blueshifts are +44.9 and +32.3 cm^{-1} in Ar and Kr, respectively, indicating stabilization of the H–Xe bond. HXeCCH has a doublet H–Xe stretching absorption measured in Xe, Kr, and Ar matrices with a splitting of 5.7, 13, and 14 cm^{-1}, respectively. *Ab initio* calculations for the 1:1 HXeCCH···Ng complexes (Ng=Ar, Kr, or Xe) are used to analyze the interaction of the hosts with the embedded molecule. These calculations support the matrix-site model where the band splitting observed experimentally is caused by specific interactions of the HXeCCH molecule with noble-gas atoms in certain local morphologies. However, the 1:1 complexation is unable to explain the observed blueshifts of the H–Xe stretching band in Ar and Kr matrices compared to a Xe matrix. More sophisticated computational approach is needed to account in detail the effects of solid environment. © *2006 American Institute of Physics*. [DOI: 10.1063/1.2221308]

I. INTRODUCTION

Since 1995 a number of noble-gas hydride molecules with the general formula HNgY (where Ng=noble-gas atom and Y=electronegative fragment) have been prepared in low-temperature matrices.[1] Preparation of these HNgY molecules involves UV photolysis of HY precursors followed by thermal mobilization of H atoms in the noble-gas host.[2,3] The first molecules prepared and characterized using this synthesis method were HXeCl, HXeBr, HXeI, and HKrCl.[1] Recent findings include HArF,[4,5] open shell species HXeO (Ref. 6) and a group of organo-noble-gas molecules prepared from acetylene and diacetylene (HXeCCH,[7,8] HXeCC,[7] HXeCCXeH,[7] HKrCCH,[9] $HXeC_4H$,[10] and $HKrC_4H$[10]). HXeCCH was first predicted computationally by Lundell *et al.* along with other large organic molecules such as Xe-insertion compounds of benzene and phenol.[11]

The HNgY molecules are high-energy metastable species with respect to the HY+Ng asymptote, and they are formed from neutral H+Ng+Y fragments.[12] Most of the significant studies on these molecules have been performed in noble-gas matrices, however, HXeI, HXeH, and HXeCl have also been reported in Xe clusters in the gas phase.[13,14] An important question concerns the existence of the HNgY molecules without the stabilizing environment of the polarizable Xe or Kr host matrix. The first HNgY molecules prepared in a different noble-gas matrix were HXeCl and HXeBr in a Kr matrix.[1] Lorenz *et al.* reported HXeCl and HXeBr in a Ne matrix and concluded from these results that these molecules should be intrinsically stable.[15] Stabilization and destabilization effects on the HXeOH molecules upon complexation with water have been studied theoretically and experimentally.[16] Due to the strong $(HNg)^+Y^-$ ion-pair character, HNgY molecules have large dipole moments and, therefore, they are attractive systems to investigate electrostatic interactions with surrounding.[3,17,18]

Recently, various computational and experimental studies on complexation of HNgY molecules have been reported.[16–23] Complexes of HXeOH with water molecules [$HXeOH\cdots H_2O$ and $HXeOH\cdots(H_2O)_2$] produce a large experimental blueshift of >100 cm^{-1} for the H–Xe stretching frequency.[16] Similarly a strong blueshifting (>100 cm^{-1}) effect was observed for the H–Kr stretching mode in the $HKrCl\cdots N_2$ complex[17,18] whereas other experimentally prepared HNgY complexes ($HArF\cdots N_2$ and $HKrF\cdots N_2$) exhibit smaller blueshifts of the H–Ng stretching vibration.[18] Stabilization of HHeF molecule upon complexation with Xe atoms was studied computationally.[20] The calculations suggested that dissociation of HHeF via the H–He stretching coordinate might be suppressed and its lifetime increased by inserting HHeF into large Xe clusters or matrices. Additionally, various 1:1 HNgY···Ng complexes have been calculated. McDowell studied computationally linear HHeF···Ng complexes[22] and in an other study, he and Buckingham compared vibrational properties of FArH···Ng and FH···Ng complexes[21] (Ng=He, Ne, Ar, and Kr). Khriachtchev *et al.* calculated 1:1 HXeBr···Xe complexes in a study of hindered rotation of HXeBr molecule.[23]

In the present work, HXeCCH molecule is made in Kr and Ar matrix media in addition to the previous studies in Xe matrices. This is the first case when the organo-noble-gas compound is prepared in an Ar matrix. The matrix effects on the H–Xe stretching absorption of HXeCCH are reported. Using calculated 1:1 HXeCCH···Ng complexes (Ng=Ar, Kr, and Xe), we analyze the interaction of the hosts with the embedded molecule. Also, experimental and computational data on acetylene-Xe complexes are presented.

[a]Electronic mail: hanna.tanskanen@helsinki.fi

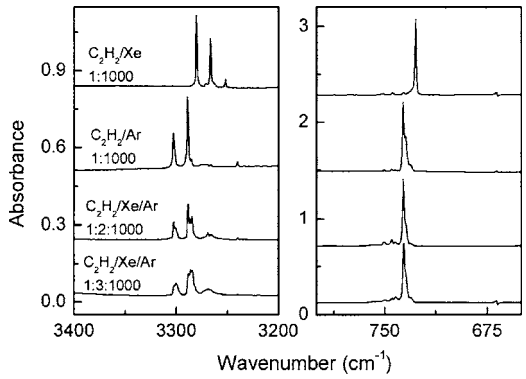

FIG. 1. IR absorption spectra of acetylene in solid Xe and Ar at 8 K (the two upper traces). Two lower traces show the effect of Xe atoms on the acetylene absorption bands in an Ar matrix.

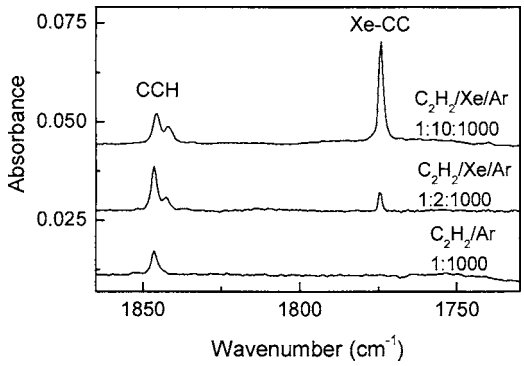

FIG. 2. IR absorption spectra in the C≡C stretching region of photolyzed C_2H_2/Xe and C_2H_2 in solid Ar at 8 K. The upper and the middle spectra correspond to 193 nm photolysis of $C_2H_2/Xe/Ar$ matrices with 3600 pulses ($\sim$10 mJ/cm^2) and 3900 pulses ($\sim$13 mJ/cm^2) and the lower spectrum is a result of the 193 nm photolysis of a C_2H_2/Ar matrix with 600 pulses ($\sim$10–14 mJ/cm^2).

II. EXPERIMENT

A. Experimental details

To prepare $C_2H_2/Xe/Ng$ (Ng=Xe, Kr, or Ar) matrices, the gases were mixed in various proportions in a glass bulb. The matrix ratios were $[C_2H_2]:[Xe]:[Ng]=1:(0–10):1000$. We used acetylene ($\geqslant$99%), Ar (Aga, $\geqslant$99.9999%), Kr (Aga, $\geqslant$99.995%), and Xe (Aga, $\geqslant$99.9990%). The samples were deposited onto a CsI window in a closed-cycle helium cryostat (DE-202, APD) at 20 K for Ar, 22–27 K for Kr, and 30 K for Xe matrices. The matrix thickness was typically $\sim$100–200 μm. The IR absorption spectra (4000–400 cm^{-1}) were recorded at 8 K using a Nicolet 60 SX Fourier transform infrared spectrometer with 1 cm^{-1} resolution coadding 500 scans. The $C_2H_2/Xe/Ng$ (Ng=Xe, Kr, or Ar) matrices were photolyzed with an excimer laser (MPB, MSX-250) operating at 193 nm (ArF).

B. Experimental results

The IR absorption spectra of acetylene in Xe and Ar matrixes (C_2H_2/Xe and C_2H_2/Ar) and in an Ar matrix doped with Xe ($C_2H_2/Xe/Ar$) are presented in Fig. 1. These spectra agree with the previous measurements of Maier and Lautz in solid Xe and Andrews *et al.* in solid Ar.[24,25] The spectra of mixed matrices ($C_2H_2/Xe/Ng$) show that Xe atoms interact with acetylene. The vibrational frequencies of acetylene in different matrix solids are presented in Table I. For the $C_2H_2\cdots Xe$ complexes, the monomer-to-complex shifts of the C–H stretching mode (ν_3) are up to −4.4 cm^{-1} in Ar and −2.0 cm^{-1} in Kr matrices. For the CC–H bending mode, only in an Ar matrix monomer-to-complex shifts are visible +5.6 and −0.2 cm^{-1}. In solid Kr, the CC–H bending absorption of acetylene becomes broader.

193 nm photolysis of a C_2H_2/Xe matrix produces mainly C_2H radicals (1852 cm^{-1}),[26] Xe–CC complexes (1767 cm^{-1}),[24] and $XeHXe^+$ ions,[27] similarly to the previous experiments.[7,28] The main photolysis products in C_2H_2/Ar and $C_2H_2/Xe/Ar$ matrices are presented in Fig. 2. It can be seen in the IR absorption spectra that the CCH radicals (monomers at 1846.5 cm^{-1} in Ar matrices)[29] interact with Xe atoms in an Ar matrix, and an additional band ($\sim$1842.5 cm^{-1}) is observed which is assigned to the $CCH\cdots Xe$ complex. Similarly upon photolysis of

TABLE I. Experimental absorptions of acetylene (in cm^{-1}). The shifts show the effect of Xe atoms in Ar and Kr matrices.

		$C_2H_2/Xe/Ar$			$C_2H_2/Xe/Kr$		
Expt. results	C_2H_2/Ar	1:2:1000	Shifts	C_2H_2/Kr	1:2:1000	Shifts	C_2H_2/Xe[a]
C–H stretch (ν_3)	3302.8	3302.8	0[b]	3293.3	3293.2	−0.1	3280.5
		3300.9	−1.8				
	3289.1	3288.7	−0.4[b]	3280.1	3280.1	0[b]	3266.5
		3286.7	−2.4		3278.1	−2.0	
		3284.7	−4.4				
($\nu_4+\nu_5$)	1334.8	1334.8	0[b]	1326.5	1326.5	0	1317
		1333	−1.8	1324.6	1324.5	−0.1	
		1330.9	−3.9				
CC–H bend (ν_5)		742.2	+5.6				
	736.8	736.6	−0.2	732.2	732.3	0	727.5
	735.1	734.9	−0.2				

[a]Values are from Ref. 28.
[b]Monomer.

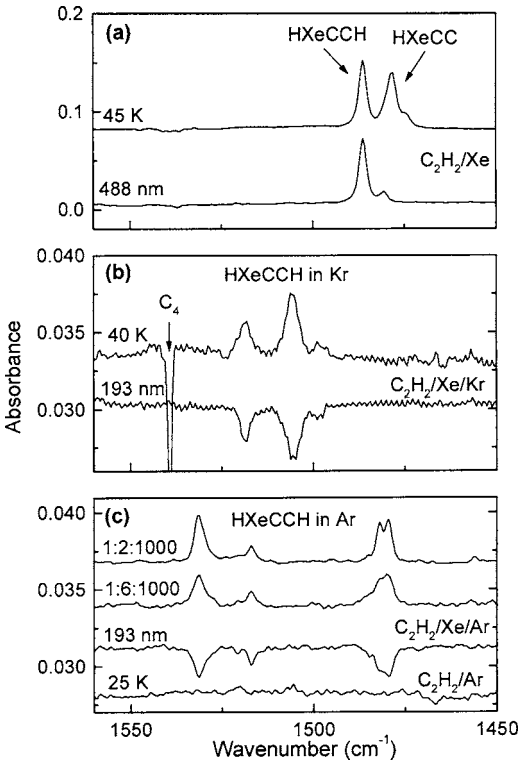

FIG. 3. IR absorption spectra of HXeCCH in the H–Xe stretching region measured in Xe (a), Kr (b), and Ar (c) matrices at 8 K. (a) The C_2H_2/Xe (1:1000) sample was first photolyzed at 193 nm and then annealed at 45 K (the upper trace). In the lower trace shown is the spectrum after 488 nm (100 mW/cm^2 for 5 min) irradiation of the annealed sample. This radiation selectively destroys HXeCC molecules. (b) The C_2H_2/Xe/Kr (1:2:1000) sample was irradiated at 193 nm and then annealed at 40 K (the upper trace). Also shown is the result of short 193 nm photolysis (20 pulses) of the annealed sample (the lower trace). (c) The C_2H_2/Xe/Ar [1:2:1000 (the first upper trace) and 1:6:1000 (the second upper trace)] samples photolyzed at 193 nm and annealed at 25 and 30 K. Also shown is the result of 20 pulses 193 nm to the annealed sample. The lowest trace shows the result of 25 K annealing of the irradiated C_2H_2/Ar (1:1000) sample demonstrating the absence of absorptions in this spectral region.

C_2H_2/Xe/Kr matrices, the CCH···Xe complex at 1844.3 cm^{-1} appears together with the CCH monomer band (1842 cm^{-1}).[28] The Xe–CC complex is also visible in the photolyzed C_2H_2/Xe/Ng matrices and its CC stretching frequencies are at 1774.3 and 1770.5 cm^{-1} in Ar and Kr matrices, respectively, corresponding to the study of Frankowski *et al.*[30]

Annealing of the photolyzed C_2H_2/Ng (Ng=Xe or Kr) matrices (at 30 K in Kr and at 45 K in Xe) mobilizes H atoms[31,32] leading to the formation of various noble-gas molecules (HXeCCH, HXeCC, HXeCCXeH, HXeH in Xe, and HKrCCH in Kr matrices).[7–9,28] IR absorption spectra of HXeCCH (Refs. 7 and 28) in solid Xe and HKrCCH (Refs. 9 and 28) in solid Kr are presented in Figs. 3(a) and 4 for the H–Ng (Ng=Xe and Kr) stretching region. In photolyzed C_2H_2/Xe/Kr samples, the annealing also yields a number of IR absorption bands. The HCC and HCC···Xe concentration increases upon annealing of the photolyzed C_2H_2/Xe/Kr matrix. In addition to the known bands of HKrCCH, C_2H_3 radicals,[33,34] and HOO radicals,[35] two unreported absorptions at 1518.7 and 1505.6 cm^{-1} and one weaker absorption at 1498.3 cm^{-1} are seen in the Xe-doped matrices [see Fig. 4 lower trace and Fig. 3(b)]. The Xe-induced bands at 1518.7, 1505.6, and 1498.3 cm^{-1} are assigned to the H–Xe stretching mode of HXeCCH in solid Kr. Annealing at 20 K of photolyzed C_2H_2/Xe/Ar matrices produces vinyl and HOO radicals similarly to Kr matrices and also four new absorptions at 1531.3, 1517.4, 1482.2, and 1479.9 cm^{-1} which are assigned to the H–Xe stretching mode of HXeCCH molecules in solid Ar. The experimental absorptions of HXeCCH in various matrix media are listed in Table II.

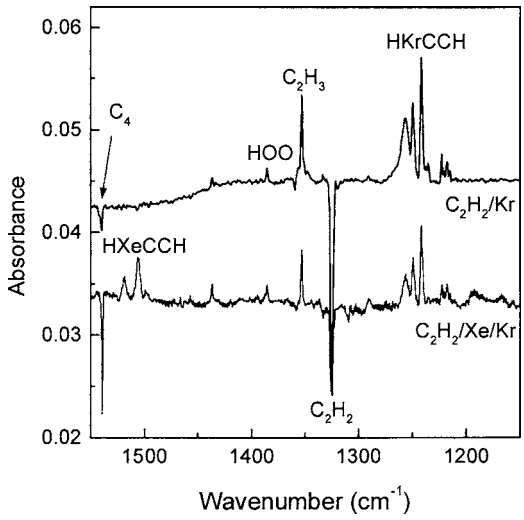

FIG. 4. Annealing-induced IR absorption spectra of HKrCCH and HXeCCH in the H–Ng stretching region measured at 8 K. The upper trace shows a typical HKrCCH spectrum in solid Kr. The C_2H_2/Kr sample was first irradiated at 193 nm and then annealed at 30 K. In the lower trace, the sample contains acetylene and Xe in solid Kr and the spectrum shows the formation of HXeCCH molecules.

III. CALCULATIONS

A. Computational details

The *ab initio* calculations of the 1:1 C_2H_2···Xe and HXeCCH···Ng (Ng=Ar, Kr, and Xe) complexes were carried out with the GAUSSIAN98 (Ref. 36) (Revision A.11.4) and GAUSSIAN03 (Ref. 37) (Revision B.02) packages of computational codes. The electron correlation methods were the Møller-Plesset second order (MP2) perturbation theory where all electrons were taken explicitly into correlation calculations (full) and the coupled clusters method [CCSD(T)] (using MP2-computed equilibrium structures). The standard split valence 6-311++G(2*d*,2*p*) basis set was applied for H, C, Ar, and Kr atoms and the effective core potential of LaJohn *et al.*[38] (LJ18) combined with Runeberg and Pyykkö's[39] valence space was employed for Xe atoms. The interaction energies of the complexes are corrected for basis set superposition error[40] (BSSE) and vibrational zero-point energy correction. The computational methods used in this study have been successfully applied for other HNgY complexes previously.[18,20,23]

B. Computational results

The structures of the 1:1 C_2H_2···Xe complexes presented in Fig. 5 are true minima on the computed potential energy surface. The complexation slightly elongates the H–C

TABLE II. Experiment IR absorptions (in cm^{-1}) of HXeCCH in different matrix media. The shifts are calculated using the strongest absorption (s) of HXeCCH in Xe.

	HXeCCH in Xe[a] (C_2H_2/Xe)	HXeCCH in Kr (C_2H_2/Xe/Kr)		HXeCCH in Ar (C_2H_2/Xe/Ar)	
			Shift		Shift
C–H stretch.	3273	···	···	···	···
H–Xe stretch	1486.4(s)	1518.7	+32.3	1531.3	+44.9
	1480.7	1505.6	+19.2	1517.4	+31
		1498.3	+11.9		
				1482.2	–4.2
				1479.9	–6.5
D–Xe stretch	1077.5	···		···	···
CC–H bend	627.6	···	···	···	···
	625.7				

[a]Values are from Refs. 28 and 7.

and C–C bonds for both structures from their values for monomeric acetylene. The calculated IR absorption frequencies and intensities are presented in Table III. The monomer-to-complex shifts of the C–H stretching mode are −3.3 and −0.9 cm^{-1} for the linear and bent complex structures, respectively. For the CC–H bending mode, the calculations show a significant difference in the monomer-to-complex shifts between these two complex structures. For the linear $C_2H_2\cdots Xe$ complex, the shift is +6.6 cm^{-1}, whereas for the bent $C_2H_2\cdots Xe$ complex it is −0.7 and −2.3 cm^{-1}. The computed interaction energies of the two stable $C_2H_2\cdots Xe$ complexes are presented in Table IV. The bent structure is energetically more favorable of the two structures by ~68 cm^{-1}.

For the 1:1 HXeCCH···Ng (Ng=Ar, Kr, and Xe) complexes, we found three configurations corresponding to the true energy minima on the computed potential energy surfaces. These configurations are similar to the reported Xe···HXeBr structures.[23] One of the structures is bent [bent (A) complex]. The other two structures are linear [linear (B) and linear (C) complexes] where the Ng atom interacts with HXeCCH from the H–Xe and C–H ends, respectively (see Fig. 6 and Table V). The complexation in the case of the bent (A) and linear (B) complexes leads to a shortening of the H–Xe bond and to an elongation of the Xe–C bond compared with the monomer. For the linear (C) complex, the complexation elongates the H–Xe bond and shortens the Xe–C bond. The changes in bond lengths between complexes and monomer are small (≤0.0009 Å). The calculated harmonic vibrational frequencies and IR absorption intensities are presented in Table VI. The complexation increases the H–Xe stretching frequency for almost all bent (A) and linear (B) complexes except for the bent Ar···HXeCCH complex. For the linear (C) complexes the complexation decreases the H–Xe stretching frequency. These complexation-induced spectral changes are similar to the previous results with the other HNgY systems.[20–23]

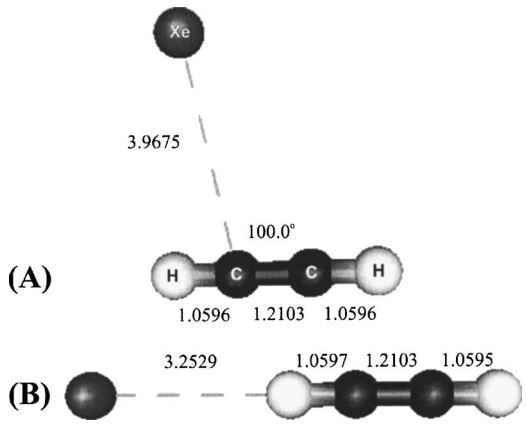

FIG. 5. Computational *ab initio* structures of the $C_2H_2\cdots Xe$ complex. The distances are in angstroms.

The computed interaction energies of the HXeCCH···Ng complexes are presented in Table VII. The bent configurations (A) of HXeCCH···Ng are energetically more favorable than the corresponding linear configurations (B) and (C) at both levels of theory. The interaction energy of the bent Xe···HXeCCH complex is largest (−444.7 cm^{-1}) and for the linear HXeCCH···Kr it is smallest (−3.0 cm^{-1}) at the MP2 level. The calculations at the CCSD(T) also show that the bent Xe···HXeCCH complex is the most strongly bound (−416.4 cm^{-1}), but the weakest bound system is the linear Ar···HXeCCH complex (−94.5 cm^{-1}). The 1:1 HXeCCH···Ng complexes are rather typical van der Waals complexes picturing a rather weak interaction between the complex moieties. This is evident also by the fact that the HXeCCH subunit structure[11] in the complex is almost unperturbed by the vicinal Xe atom, and the molecular partial charges change very little. A slight increase of ionicity in the general nature of HXeCCH is, however, found.

IV. DISCUSSION

In the experiments, we used acetylene and Xe as precursors in solid Kr and Ar. Figure 1 shows the effect of doping with Xe atoms on the acetylene spectra in solid Ar. The Xe doping produces new spectral features for C_2H_2, which is due to $C_2H_2\cdots Xe$ complexation, and the H–Xe stretching complexation-induced bands are redshifted from the C_2H_2 monomer bands in both Ar and Kr matrices. The proportion of the $C_2H_2\cdots Xe$ complexes is larger for Ar than for Kr

TABLE III. Computational spectra of C_2H_2 monomer and $C_2H_2\cdots Xe$ complexes at the MP2(full) level of theory. The vibrational frequencies are in cm^{-1} and IR intensities (in parentheses) are in km mol^{-1}. The shifts are calculated subtracting the frequencies of complex from the value of monomer.

Computational results	C_2H_2	$C_2H_2\cdots Xe$		$C_2H_2\cdots Xe$	
		Linear complex	Shifts	Bent complex	Shifts
	3534.2 (0)	3530.9 (2)		3532.9 (0)	
C–H stretch (ν_3)	3447.0 (92)	3443.7 (139)	−3.3	3446.1 (89)	−0.9
CC stretch	1965.4 (0)	1963.8 (1)		1963.8 (0)	
CC–H bend (ν_5)	738.1 (100)[a]	744.7 (86)[a]	+6.6	737.4 (90)	−0.7
				735.8 (114)	−2.3
	592.0 (0)[a]	599.5 (1)[a]		589.9 (0)	
				579.9 (0)	
		37.4 (0)		43.2 (0)	
		34.5 (0)[a]		19.3 (0)	

[a]Degenerated bending modes.

matrices, i.e., the complexation of C_2H_2 with Xe atoms is more efficient in Ar matrices. This is probably due to competing "complexation" with host atoms, which is presumably stronger for Kr than for Ar. The experimental shifts of the C–H stretching vibration are up to −4.4 cm^{-1} in Ar matrices and −2.0 cm^{-1} in Kr matrices, which agree with the calculations for the 1:1 $C_2H_2\cdots Xe$ complexes. The computed C–H stretching absorption shifts are −0.9 cm^{-1} for the bent $C_2H_2\cdots Xe$ complex and −3.3 cm^{-1} for the linear $C_2H_2\cdots Xe$ complex. For the CC–H bending mode, the observed experimental shifts are +5.6 and −0.2 cm^{-1} in Ar matrices and no shift is observed in Kr matrices. For the bent $C_2H_2\cdots Xe$ complex, the calculated shift of the CC–H bending mode is −0.7 and −2.3 cm^{-1} for the two split components, which basically agree with the experimental results. For the linear $C_2H_2\cdots Xe$ complex, the calculations give a blueshifted value (+6.6 cm^{-1}) for the CC–H bending mode, which is very close to the measured experimental value in an Ar matrix. This suggests that both configurations of $C_2H_2\cdots Xe$ are present in the matrix, even though the bent configuration is energetically more favorable of the two structures. In literature, several experimental and computational studies on $C_2H_2\cdots Ng$ (Ng=He, Ne, and Ar) complexes can be found. The calculations of Hasse *et al.* gave for $C_2H_2\cdots Ar$ complex T-shaped structures,[41] and in a recent study, Munteanu and Fernández have calculated intermolecular ground-state potential energy surfaces of the $C_2H_2\cdots He$, Ne, and Ar van der Waals complexes.[42] Rutkowski *et al.* studied acetylene dissolved in liquefied Kr, Ar, N_2, CO, and CO_2 using IR absorption measurements and B3LYP and MP2 calculations.[43] Their calculations predicted minima for the $C_2H_2\cdots B$ (B =Ar, N_2, CO, and CO_2) linear structures. The IR spectra of these systems suggest an increasing effect of anisotropic intermolecular interactions in the molecular solvent.[43] Lorenz *et al.* have studied experimentally and computationally HBr···Xe and HCl···Xe complexes, which were observed after deposition of HBr/Xe and HCl/Xe samples in solid Ne.[15] These HBr···Xe and HCl···Xe complexes were the precursors of HXeBr and HXeCl molecules in solid Ne, similarly to the present study, where the acetylene-Xe complexes are the precursors of HXeCCH.

The 193 nm photolysis of acetylene-Xe complex in Kr and Ar matrices yields HCC radicals and its complexes with Xe and also Xe–CC molecules (see Fig. 2). The HCC···Xe complexes are more visible in solid Ar than in solid Kr, i.e., the complexation with Xe is stronger in Ar matrices. This trend is in agreement with better C_2H_2–Xe complexation in Ar matrix. The photolyzed C_2H_2/Xe/Ng matrices were annealed to mobilize the H atoms in the lattice. The annealing makes possible the formation of HXeCCH molecules in the H+HCC···Xe reaction in Ar and Kr matrices. The HCC···Ng complex was not calculated because the results at the computational level used here could be unreliable for the open shell species.

The assignment of the observed novel bands to

TABLE IV. MP2-computed interaction energies of the $C_2H_2\cdots Xe$ complex structures. The values are in cm^{-1}.

	$C_2H_2\cdots Xe$ (bent)	$C_2H_2\cdots Xe$ (linear)
E_{int}	−226.2	−220.6
$E_{int,ZPVE}$[a]	−205.5	−157.4
$E_{int,CP}$[b]	−161.5	−135.8
$E_{int,CP\text{-}ZPVE}$	−140.8	−72.6

[a]Zero-point vibrational energy corrected interaction energy.
[b]Counterpoise corrected interaction energy taking into account the BSSE energy contribution.

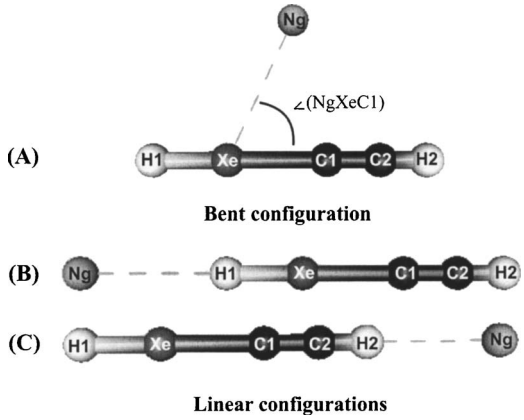

FIG. 6. Computational structures of the HXeCCH···Ng complex. The geometry parameters calculated are presented in Table V.

TABLE V. Computational geometries of the HXeCCH monomer and the HXeCCH···Ng complexes obtained at the MP2(full) level. The notation of atoms is shown in Fig. 6. The angles are in degrees and the distances are in Å.

	Bent Ng complex (A)								
	∠(NgXeCl)	∠(H1XeCl)	∠(XeC1C2)	∠(C1C2H2)	*r*(NgXe)	*r*(H1Xe)	*r*(XeC1)	*r*(C1C2)	*r*(C2H2)
HXeCCH···Ar	67.9	180.0	179.51	179.91	3.9733	1.7585	2.3066	1.2268	1.0624
HXeCCH···Kr	67.3	179.98	179.01	179.83	4.0162	1.7582	2.3070	1.2270	1.0624
HXeCCH···Xe	65.7	179.98	178.94	179.80	4.1468	1.7577	2.3080	1.2272	1.0625
	Linear Ng complex (B)								
	r(NgH1)	*r*(H1Xe)	*r*(XeC1)	*r*(C1C2)	*r*(C2H2)				
Ar···HXeCCH	3.4032	1.7580	2.3073	1.2268	1.0623				
Kr···HXeCCH	3.3635	1.7576	2.3079	1.2268	1.0623				
Xe···HXeCCH	3.3687	1.7581	2.3089	1.2268	1.0623				
	Linear Ng complex (C)								
	r(H2Ng)	*r*(H1Xe)	*r*(XeC1)	*r*(C1C2)	*r*(C2H2)				
HXeCCH···Ar	3.0089	1.7588	2.3064	1.2268	1.0621				
HXeCCH···Kr	3.0573	1.7589	2.3063	1.2268	1.0621				
HXeCCH···Xe	3.2462	1.7590	2.3062	1.2270	1.0623				
	Monomer								
	r(H1Xe)	*r*(XeC1)	*r*(C1C2)	*r*(C2H2)					
HXeCCH	1.7586	2.3066	1.2267	1.0623					

HXeCCH molecules in Ar and Kr matrices is based on several experimental facts. The additional bands presented in Table II appear in Ar and Kr matrices only when Xe atoms are added to the gas mixture [see Figs. 3(c) and 4]. These bands are formed upon annealing of the photolyzed matrices containing the HCC···Xe species. In principle, this Xe-containing species could also be HXeCC because Xe–CC (precursor of HXeCC) is seen in the photolyzed matrices and the absorptions of HXeCCH and HXeCC are located in the same spectral region.[7] As the most probable candidate, we consider HXeCCH molecules rather than HXeCC radicals. For instance, HXeCCH and HXeCC can be distinguished from their different photostabilities.[7,28] The HNgY molecules usually decompose easily upon irradiation in UV and in some cases in visible spectral regions.[2,7,9,16] In the present case, the Xe-containing species in Kr and Ar decompose efficiently after 20 pulses (~10 mJ/cm^2) at 193 nm (see Fig. 3), which is similar to HXeCCH in solid Xe. We irradiated the photolyzed and annealed (C_2H_2/Xe/Ar) sample at 488 nm from an Ar^+ laser (~100 mW/cm^2 for 5 min). The species under discussion is stable under 488 nm irradiation, which is characteristic for HXeCCH whereas HXeCC is efficiently bleached by 488 nm radiation in 1 min time scale [see Fig. 3(a)].[7,28] It was found in Xe matrices that the HXeCCH to HXeCC proportion strongly depends on the 193 nm photolysis time of the deposited matrices.[7] We used different photolysis periods for the C_2H_2/Xe in Ar and Kr matrices; however, this did not change the relative intensities of the annealing-induced bands shown in Fig. 3. These facts indicate that all bands in this region belong to the same absorber (HXeCCH). The CCH bending and CH stretching absorptions were not observed in the mixed matrices because they were too weak and they could not be used to distinguish between HXeCCH and HXeCC.

It is not absolutely clear why HXeCC radicals are not observed in these experiments; however, several reasons exist. First, we used photolysis at 193 nm, which was previously found to favor the HXeCCH formation.[7] Second, photolysis of C_2H_2 and CCH can be a local process,[44] and the formation of H_2 molecules can take place upon photodecomposition of CCH radicals. If H_2 molecules form upon photolysis, the formation of HXeCC needs global mobility of H atoms, which can be somewhat suppressed in the mixed matrices. Third, the Xe–CC molecule is computationally bent (148.6°),[30] which can produce a barrier for the formation of a linear HXeCC molecule, and this slows down the reaction at lower annealing temperatures in Ar and Kr matrices. We observed in solid Kr (C_2H_2/Xe/Kr) that the HCC and HCC···Xe concentrations increase upon annealing. In the C_2H_2/Xe experiments, HCC and Xe–CC form during photolysis but annealing decreases the amount of these compounds because HCC and Xe–CC are the precursors for HXeCCH and HXeCC, respectively.[7,45] The observed increase of the HCC···Xe concentration during annealing in solid Kr shows that H atoms can react with XeCC molecules without the formation of HXeCC. It seems that an H atom reacts more likely with C than with Xe atoms of Xe–CC molecules, which leads to the HCC···Xe complexes.

Two H–Xe stretching bands of HXeCCH are observed in solid Xe [see Fig. 3(a), the lower trace].[28] The doublet structure of the H–Ng stretching mode is characteristic for the HNgY molecules,[3,23] as seen, for example, in the case of

TABLE VI. Calculated MP2(full)/LJ18(Xe),6-311++G(2*d*,2*p*) vibrational frequencies (in cm^{-1}) and IR intensities shown in parentheses (in km mol^{-1}) of the HXeCCH···Ng complexes. The shifts are calculated subtracting the frequencies of complex from the value of monomer.

	Ar···HXeCCH [bent (A)]		Ar···HXeCCH [linear (B)]		HXeCCH···Ar [linear (C)]	
		Shift		Shift		Shift
C–H stretch	3453.8 (32)	−0.7	3454.3 (32)	−0.2	3457.8 (51)	+3.3
C–C stretch	1956.1 (11)	−1.1	1956.9 (11)	−0.3	1957.1 (14)	−0.1
H–Xe stretch	1694.2 (1086)	−0.1	1700.7 (1102)	+6.4	1693.1 (1140)	−1.2
Bend	672.7 (24)	−0.4	676.0 (23)[a]	+2.9	675.5 (42)[a]	+2.4
	672.4 (25)	−0.7				
Bend	650.1 (29)	−0.7	651.2 (33)[a]	+0.4	662.8 (10)[a]	+12.0
	648.2 (32)	−2.6				
Xe–C stretch	332.0 (143)	−0.1	331.7 (152)	−0.4	333.6 (146)	+1.5
H–Xe–C bend	131.9 (13)	+1.6	130.3 (12)	0	135.8 (11)[a]	+5.5
	129.5 (12)	−0.8	129.5(12)	−0.8		
	35.5 (0)		19.2 (0)		27.2 (0)	
	24.6 (1)		6.8 (1)		15.5 (1)[a]	
	Kr···HXeCCH [bent (A)]		Kr···HXeCCH [linear (B)]		HXeCCH···Kr [linear (C)]	
		Shift		Shift		Shift
C–H stretch	3453.3 (32)	−1.2	3454.2 (32)	−0.3	3456.3 (63)	+1.8
C–C stretch	1955.4 (11)	−1.8	1956.7 (12)	−0.5	1956.9 (16)	−0.3
H–Xe stretch	1694.4 (1065)	+0.1	1703.7 (1111)	+9.4	1692.9 (1162)	−1.4
Bend	672.4 (24)	−0.7	680.6 (20)[a]	+7.5	690.4 (46)	+17.3
	671.6 (25)	−1.5				
Bend	649.8 (28)	−1.0	651.4 (35)[a]	+0.6	669.1 (2)[a]	+18.3
	645.6 (34)	−5.2				
Xe–C stretch	331.8 (140)	−0.3	331.4 (159)	−0.7	334.2 (147)	+2.1
H–Xe–C bend	131.4 (13)	+1.1	131.0 (13)[a]	+0.7	140.3 (10)[a]	+10.0
	129.4 (11)	−0.9				
	35.9 (0)		19.8 (0)		24.6 (0)	
	26.6 (0)		10.5 (1)[a]		20.8 (2)[a]	
	Xe···HXeCCH [bent (A)]		Xe···HXeCCH [linear (B)]		HXeCCH···Xe [linear (C)]	
		Shift		Shift		Shift
C–H stretch	3452.7 (32)	−1.8	3454.1 (32)	−0.4	3454.2 (72)	−0.2
C–C stretch	1954.0 (11)	−3.2	1956.3 (13)	−0.9	1955.6 (18)	−1.6
H–Xe stretch	1695.2 (1045)	+0.9	1697.8 (1122)	+3.5	1692.5 (1191)	−1.8
Bend	672.0 (23)	−1.1	677.0 (22)[a]	+3.9	678.1 (44)[a]	+5.0
	671.3 (28)	−1.8				
Bend	649.7 (28)	−1.1	651.1 (33)[a]	+0.3	666.4 (1)[a]	+15.6
	647.6 (33)	−3.2				
Xe–C stretch	331.2 (137)	−0.9	330.6 (171)	−1.5	334.1 (151)	+2.0
H–Xe–C bend	132.6 (15)	+2.3	129.8 (13)[a]	−0.5	134.2 (10)	+3.9
	129.1 (11)	−1.2			130.5 (11)	−0.2
	40.4 (1)		19.9 (0)		21.0 (0)	
	27.7 (0)		4.6 (1)		14.5 (1)	
	HXeCCH (monomer)					
C–H stretch	3454.5 (32)					
C–C stretch	1957.2 (11)					
H–Xe stretch	1694.3 (1111)					
Bend	673.1 (26)[a]					
Bend	650.8 (30)[a]					
Xe–C stretch	332.1 (146)					
H–Xe–C bend	130.3 (12)[a]					

[a]Degenerated bending modes.

HXeI, HXeBr, HXeCN, HXeSH, HKrCN, and HKrCl.[1–3,46,47] In addition, somewhat different shapes of the H–Ng stretching absorption bands have also been observed. A number of organo-noble-gas molecules (HXeCCXeH, HKrCCH, $HXeC_4H$, and $HKrC_4H$) show a more extensive H–Ng stretching band fine structure (up to five different ab-

TABLE VII. Electronic interaction energies and vibrational BSSE and ZPVE-corrected electronic interaction energies of the Ng···HXeCCH complexes obtained at MP2 level. The values are in cm^{-1}.

	Ar···HXeCCH [bent (A)]	Ar···HXeCCH [linear (B)]	HXeCCH···Ar [linear (C)]
$E_{int(MP2)}$	−305.8	−106.2	−164.0
$E_{int[CCSD(T)]}$[a]	−207.4	−94.5	−164.7
$E_{int,CP(MP2)-ZPVE}$	−153.4	−38.3	−12.9
	Kr···HXeCCH [bent (A)]	Kr···HXeCCH [linear (B)]	HXeCCH···Kr [linear (C)]
$E_{int(MP2)}$	−471.4	−193.8	−271.7
$E_{int[CCSD(T)]}$[a]	−335.8	−164.1	−256.3
$E_{int,CP(MP2)-ZPVE}$	−249.5	−16.2	−3.0
	Xe···HXeCCH [bent (A)]	Xe···HXeCCH [linear (B)]	HXeCCH···Xe [linear (C)]
$E_{int(MP2)}$	−627.5	−249.8	−242.2
$E_{int[CCSD(T)]}$[a]	−416.4	−194.6	−215.2
$E_{int,CP(MP2)-ZPVE}$	−444.7	−168.4	−106.0

[a]MP2-computed equilibrium structures are used in calculations.

sorptions), which has been explained by the matrix-site effect.[9,10,28] The most detailed study has recently addressed the doublet structure of the HXeBr molecule.[23] It was concluded that the doublet of the main spectral feature of HXeBr is described as matrix sites due to specific interactions with noble-gas atoms in well-defined local matrix morphologies. For HXeBr the observed splitting between H–Xe stretching components was about 3.5 cm^{-1} and calculations on the 1:1 Xe···HXeBr complexes showed that the interaction can change the H–Xe stretching frequency by several cm^{-1}.[23] For HXeCCH in solid Xe, the interval between two H–Xe stretching bands is 5.7 cm^{-1}. Our calculations on 1:1 HXeCCH···Xe complexes give spectral shifts up to 5.3 cm^{-1} and the splitting can be explained by specific interactions of the HXeCCH molecule with Xe atoms in certain local morphologies. The present results are consistent with the conclusions of Ref. 28 that the two close H–Xe stretching bands are attributed to matrix sites. A similar doublet in the H–Xe stretching region is visible for HXeCCH in Kr and Ar matrices as well [see Figs. 3(b) and 3(c), respectively]. The experimental splitting of the H–Xe stretching doublet of HXeCCH is ~13 cm^{-1} in solid Kr and ~14 cm^{-1} in solid Ar. The calculations on the H–Xe stretching mode of 1:1 HXeCCH···Kr and HXeCCH···Ar complexes show that the H–Xe stretching frequency can vary up to 10.8 and 7.6 cm^{-1} depending on structures of the HXeCCH···Kr and HXeCCH···Ar complexes, respectively. The observed splitting in solid Kr is quite close to the computed value on the HXeCCH···Kr complexes, but the correspondence between experiments and calculations is worse in the case of Ar, however, being still acceptable. Furthermore, the calculations describe 1:1 complexes in a vacuum whereas the experiments are performed in the solid phase, and the solid surrounding can modify the geometry and the relative energies of the interactive molecular systems. The increase of the Xe/Ng ratio broadens the H–Xe absorption bands as it is seen in Fig. 3(c), which could be explained by a change of matrix morphology. This effect was seen also previously in systems such as $HKrCl···N_2$ in solid Kr (Ref. 17) and HXeBr in solid Xe,[23] but the atomistic level mechanisms behind these observations are still unresolved.

The matrix effects generally include not only relatively small matrix-site splittings but also larger matrix-induced shifts due to more extensive interactions with the matrix material described as solvation effects.[48] In our case, HXeCCH molecule can interact with different lattice atoms depending the host matrix material (Xe, Kr, and Ar). For the H–Xe stretching absorptions, the highest frequency is found in solid Ar (1531.3 cm^{-1}) and it is almost 13 cm^{-1} higher than that obtained in solid Kr and ~45 cm^{-1} higher than that in solid Xe. This indicates that the stabilization of the H–Xe stretching bond is stronger in Ar than in Kr or Xe matrices. We try to understand if a single atom interaction to HXeCCH molecule could explain the observed shifts between HXeCCH in Xe and HXeCCH in other matrix media (Kr or Ar). The calculations performed on the 1:1 HXeCCH···Ng (Ng=Ar, Kr, and Xe) complexes show that the interaction energies for these systems are small (maximum −444.7 cm^{-1}) and the computational complexation-induced spectral shifts are quite different from the obtained solvation effect. It can be seen in Table VI that the computed complexation-induced shifts vary from −1.2 to +6.4 cm^{-1}, from −1.4 to +9.4 cm^{-1}, and from −1.8 to +3.5 cm^{-1} for HXeCCH···Ar, HXeCCH···Kr, and HXeCCH···Xe complexes depending on the configuration, respectively. The calculations give the most blueshifted value for the H–Xe stretching vibration of the linear Kr···HXeCCH complex (B), whereas the largest experimental blueshift is found in an Ar matrix (see Table II). This means that the calculations on the 1:1 complexes are relevant to the matrix-site structure of HXeCCH as discussed above, but they are unable to describe the observed shift of HXeCCH between various matrix materials. To describe the solvation effect, the calculations should be done for much bigger HXeCCH···$(Ng)_n$ systems, and even dynamical effects should be probably included. The previous studies on HXeCl, HXeBr, and HXeCN molecules prepared in solid Kr are comparable with our present results.[1,46] The H–Xe stretching absorption of HXeCl measured in solid Kr is shifted by +15 cm^{-1} as compared to Xe matrices and this shift is +20 cm^{-1} for HXeBr and +26 cm^{-1} for HXeCN. For HXeCCH in solid Kr, the maximum shift of

the H–Xe stretching frequency is +32.3 cm^{-1} from the value in solid Xe. It should be noted that in solid Ar, we also observed redshifted (4–6 cm^{-1}) absorption bands as compared with solid Xe (see Table II). The redshifted bands possibly originate from the presence of vicinal vacancies. As an exciting observation, Lorenz *et al.*[15] have prepared HXeCl and HXeBr molecules in solid Ne. In their study, the H–Xe stretching absorption bands of HXeCl and HXeBr measured were redshifted by ~−36 and −54 cm^{-1} from the values in Xe matrices, respectively. It is unclear at the moment why the H–Xe stretching frequencies increase in Ar and Kr matrices and decrease in Ne matrices compared to Xe matrices. The computational efforts to model the trapping site effect on the atomistic level by including more Xe atoms in the quantum chemical model applied here, by combined QM/MM or classical MD simulations, are beyond this study and represent a challenge for the computations in the future.

V. CONCLUSIONS

HXeCCH molecules were prepared from C_2H_2 and Xe in solid Kr and Ar matrices and characterized by IR absorption spectroscopy. The experimental data show that HXeCCH can form in other surroundings than a polarizable Xe environment. Two new annealing-induced absorptions were found at 1518.7 and 1505.6 cm^{-1} and one weaker absorption at 1498.3 cm^{-1} in solid Kr and four new absorptions at 1531.3, 1517.4, 1482.2, and 1479.9 cm^{-1} in solid Ar, which are all assigned to the H–Xe stretching mode of HXeCCH molecules. The H–Xe stretching absorptions of HXeCCH in Ar and Kr are blueshifted from the value measured in solid Xe. The maximum blueshift is +44.9 cm^{-1} in Ar and +32.3 cm^{-1} in Kr matrices indicating that the stabilization of this bond is stronger in Ar than in Kr or Xe matrices, which is a remarkable and novel observation. We have previously observed two H–Xe stretching bands of HXeCCH in solid Xe with an interval of 5.7 cm^{-1}.[28] A similar doublet is visible for HXeCCH in solid Kr and Ar with intervals of ~13 and ~14 cm^{-1}, respectively. Calculations were performed on the 1:1 HXeCCH···Ng complexes (Ng=Ar, Kr, or Xe) at the MP2 and CCSD(T) levels and three stable configurations (one bent and two linear structures) were found. The calculations on the HXeCCH···Xe complexes give spectral shifts up to 5.3 cm^{-1} between H–Xe stretching vibrations and in the case of HXeCCH···Kr and HXeCCH···Ar complexes the H–Xe frequency can vary up to 10.8 and 7.6 cm^{-1} depending on the structure of complex, respectively. The calculations support the matrix-site model where the band splitting is caused by specific interactions of the HXeCCH molecule with the Ng atoms in certain local morphologies. However, the 1:1 complexation is unable to explain the observed blueshifts of the H–Xe stretching band in Ar and Kr matrices compared to a Xe matrix. More extensive theoretical work is needed to account the effects of solid environment in more detail.

ACKNOWLEDGMENTS

The Academy of Finland supported this work. The CSC-Center for Scientific Computing Ltd. (Espoo, Finland) is thanked for computer resources. We thank Antti Lignell for useful discussions on calculations and Susanna Johansson for help in experiments.

[1] M. Pettersson, J. Lundell, and M. Räsänen, J. Chem. Phys. **102**, 6423 (1995).
[2] M. Pettersson, L. Khriachtchev, J. Lundell, and M. Räsänen, *Inorganic Chemistry in Focus II*, edited by G. Meyer, D. Naumann, and L. Wesemann (Wiley-VCH, New York, 2005), pp. 15–34.
[3] J. Lundell, L. Khriachtchev, M. Pettersson, and M. Räsänen, Low Temp. Phys. **26**, 680 (2000).
[4] L. Khriachtchev, M. Pettersson, N. Runeberg, J. Lundell, and M. Räsänen, Nature (London) **406**, 874 (2000).
[5] L. Khriachtchev, M. Pettersson, A. Lignell, and M. Räsänen, J. Am. Chem. Soc. **123**, 8610 (2001).
[6] L. Khriachtchev, M. Pettersson, J. Lundell, H. Tanskanen, T. Kiviniemi, N. Runeberg, and M. Räsänen, J. Am. Chem. Soc. **125**, 1454 (2003).
[7] L. Khriachtchev, H. Tanskanen, J. Lundell, M. Pettersson, H. Kiljunen, and M. Räsänen, J. Am. Chem. Soc. **125**, 4696 (2003).
[8] V. I. Feldman, F. F. Sukhov, A. Y. Orlov, and I. V. Tyulpina, J. Am. Chem. Soc. **125**, 4698 (2003).
[9] L. Khriachtchev, H. Tanskanen, A. Cohen, R. B. Gerber, J. Lundell, M. Pettersson, H. Kiljunen, and M. Räsänen, J. Am. Chem. Soc. **125**, 6876 (2003).
[10] H. Tanskanen, L. Khriachtchev, J. Lundell, H. Kiljunen, and M. Räsänen, J. Am. Chem. Soc. **125**, 16361 (2003).
[11] J. Lundell, A. Cohen, and R. B. Gerber, J. Phys. Chem. A **106**, 11950 (2002).
[12] M. Pettersson, J. Nieminen, L. Khriachtchev, and M. Räsänen, J. Chem. Phys. **107**, 8423 (1997).
[13] R. Baumfalk, N. H. Nahler, and U. Buck, J. Chem. Phys. **114**, 4755 (2001).
[14] N. H. Nahler, M. Fárnik, and U. Buck, J. Chem. Phys. **301**, 173 (2004).
[15] M. Lorenz, M. Räsänen, and V. E. Bondybey, J. Phys. Chem. A **104**, 3770 (2000).
[16] A. V. Nemukhin, B. L. Grigorenko, L. Khriachtchev, H. Tanskanen, M. Pettersson, and M. Räsänen, J. Am. Chem. Soc. **124**, 10706 (2002).
[17] A. Lignell, L. Khriachtchev, M. Pettersson, and M. Räsänen, J. Chem. Phys. **117**, 961 (2002).
[18] A. Lignell, L. Khriachtchev, M. Pettersson, and M. Räsänen, J. Chem. Phys. **118**, 11120 (2003).
[19] S. A. C. McDowell, Phys. Chem. Chem. Phys. **5**, 808 (2003).
[20] A. Lignell, L. Khriachtchev, M. Räsänen, and M. Pettersson, Chem. Phys. Lett. **390**, 256 (2004).
[21] S. A. C. McDowell and A. D. Buckingham, Spectrochim. Acta, Part A **61**, 1603 (2005).
[22] S. A. C. McDowell, J. Mol. Struct.: THEOCHEM **715**, 73 (2005).
[23] L. Khriachtchev, A. Lignell, J. Juselius, M. Räsänen, and E. Savchenko, J. Chem. Phys. **122**, 014510 (2005).
[24] G. Maier and C. Lautz, Eur. J. Org. Chem., 769 (1998).
[25] L. Andrews, G. L. Johnson, and B. J. Kensall, J. Phys. Chem. **86**, 3374 (1982).
[26] D. Forney, M. E. Jacox, and W. E. Thomson, J. Mol. Spectrosc. **170**, 178 (1995).
[27] H. Kunttu, J. Seetula, M. Räsänen, and V. A. Apkarian, J. Chem. Phys. **96**, 5630 (1992).
[28] H. Tanskanen, L. Khriachtchev, J. Lundell, and M. Räsänen, J. Chem. Phys. **121**, 8291 (2004).
[29] D. E. Milligan, M. E. Jacox, and L. Abouaf-Marguin, J. Chem. Phys. **46**, 4562 (1967).
[30] M. Frankowski, A. M. Smith-Gicklhorn, and V. E. Bondybey, Can. J. Chem. **82**, 837 (2004).
[31] J. Eberlein and M. Creutzburg, J. Chem. Phys. **106**, 2188 (1997).
[32] L. Khriachtchev, H. Tanskanen, M. Pettersson, M. Räsänen, V. Feldman, F. Sukhov, A. Orlov, and A. F. Shestakov, J. Chem. Phys. **116**, 5708 (2002).
[33] R. A. Shepherd, T. J. Doyle, and W. R. M. Graham, J. Chem. Phys. **89**, 2738 (1988).
[34] H. Tanskanen, L. Khriachtchev, M. Räsänen, V. I. Feldman, F. F. Sukhov, A. Yu. Orlov, and D. A. Tyurin, J. Chem. Phys. **123**, 064318 (2005).
[35] D. Milligan and M. Jacox, J. Chem. Phys. **38**, 2627 (1963).
[36] M. J. Frisch, G. W. Trucks, H. B. Schlegel *et al.*, GAUSSIAN 98, Revision A.11.4, Gaussian, Inc., Pittsburgh, PA, 2002.

[37] M. J. Frisch, G. W. Trucks, H. B. Schlegel *et al.*, GAUSSIAN 03, Revision B.02, Gaussian, Inc., Pittsburgh, PA, 2003.
[38] L. A. LaJohn, P. A. Christiansen, R. B. Ross, T. Atashroo, and W. C. Elmer, J. Chem. Phys. **87**, 2812 (1987).
[39] N. Runeberg and P. Pyykkö, Int. J. Quantum Chem. **66**, 131 (1998).
[40] S. F. Boys and F. Bernardi, Mol. Phys. **19**, 553 (1970).
[41] R. D. Hasse, M. W. Severson, M. M. Szczesniak, G. Chalasinski, P. Cieplak, R. A. Kendall, and S. M. Cybulski, J. Mol. Struct. **436**, 387 (1997).
[42] C. R. Munteanu and B. Fernández, J. Chem. Phys. **123**, 014309 (2005) and references therein.
[43] K. S. Rutkowski, S. M. Melikova, D. A. Smirnov, P. Rodziewicz, and A. Koll, J. Mol. Struct. **614**, 305 (2002).
[44] L. Khriachtchev, M. Pettersson, J. Lundell, and M. Räsänen, J. Chem. Phys. **114**, 7727 (2001).
[45] V. I. Feldman, F. F. Sukhov, A. Yu. Orlov, I. V. Tyulpina, E. A. Logacheva, and D. A. Tyurin, Russ. Chem. Bull. **54**, 1458 (2005).
[46] M. Pettersson, J. Lundell, L. Khriachtchev, and M. Räsänen, J. Chem. Phys. **109**, 618 (1998).
[47] M. Pettersson, J. Lundell, L. Khriachtchev, E. Isoniemi, and M. Räsänen, J. Am. Chem. Soc. **120**, 7979 (1998).
[48] A. J. Barnes, *Vibrational Spectroscopy of Trapped Species*, edited by H. E. Hallam (Wiley, London, 1973), p. 133.